ADVANCED MATERIALS TECHNOLOGIES
www.advmattechnol.de

Microscopic Softening Mechanisms of an Ionic Liquid Additive in an Electrically Conductive Carbon-Silicone Composite

Long Zhang, Dominik S. Schmidt, Lola González-García, and Tobias Kraus**

The microstructural changes caused by the addition of the ionic liquid (IL) 1-ethyl-3-methylimidazolium bis(trifluoromethylsulfonyl)imide to polydimethylsiloxane (PDMS) elastomer composites filled with carbon black (CB) are analyzed to explain the electrical, mechanical, rheological, and optical properties of IL-containing precursors and composites. Swelling experiments and optical analysis indicate a limited solubility of the IL in the PDMS matrix that reduces the cross-linking density of PDMS both globally and locally, which reduces the Young's moduli of the composites. A rheological analysis of the precursor mixture shows that the IL reduces the strength of carbon–carbon and carbon–PDMS interactions, thus lowering the filler–matrix coupling and increasing the elongation at break. Electromechanical testing reveals a combination of reversible and irreversible piezoresistive responses that is consistent with the presence of IL at microscopic carbon–carbon interfaces, where it enables re-established electrical connections after stress release but reduces the absolute conductivity.

1. Introduction

Conductive elastomer composites (CECs) with electrically conductive fillers such as carbon or metal particles in an insulating polymer matrix have found application as flexible electrodes, actuators, and sensors.[1–8] Silicone composites (often based on polydimethylsiloxane, PDMS) are commonly used in stretchable electronics.[9–12] The ideal CECs would sustain large deformations while remaining conductive and mechanically stable during many cycles. The electrical conductivity of the undeformed composites increases with the filling ratio, and the relative drop in conductivity upon deformation tends to decrease with number of conductive pathways.[13] The formation of conductive pathways is promoted by high aspect ratio fillers (i.e., carbon nanotubes [CNTs], graphene) and filling ratios above the percolation threshold.

Carbon black (CB) is widely used as filler due to its commercial availability and low price. The fractal-shaped carbon aggregates in CB are non-uniform and their interaction in the polymer is often unknown. The CB aggregates are branched and have a fractal dimension that is closer to three than to one, in contrast to the almost linear CNTs. Higher CB than CNT filling ratios are required to sufficiently exceed the percolation threshold,[14] which leads to stiff and brittle composites and highly viscous precursors that are difficult to process.

Alternative approaches include soft block copolymers,[15,16] mixtures of conductive polymers with elastomers,[17–19] and stretchable conductors based on biogenic polymers such as cellulose filled with conductive carbon fibers or CNTs.[20–22] Some of them are prepared using considerable amounts of solvents, others use costly or less common precursors, which explains their small market shares.

Solid carbon and metal particles remain highly popular conductive fillers for CECs. Such fillers reduce the elasticity of elastomer composites at high filling ratios,[23] which limits their application in soft robotics, wearables, and implants, for example. Additives were introduced that tune filler–polymer interfaces and change the elastomer network to improve the mechanical properties of elastomer composites and engineer their electrical response to strain. Certain ionic liquids (IL) modify the dispersion state of the fillers and change bulk material properties.[24–28] Hassouneh et al. reported the use of 1-ethyl-3-methylimidazolium bis(trifluoromethanesulfonyl) imide [EMIM][TFSI] in PDMS/CNT composites with detailed data on the conductivity change depending on mixing sequence and method.[29] The authors found the highest bulk conductivity of 5–10 S m^{-1} for the elastomer composites where IL was used to disperse the CNT fillers combined with effective mechanical mixing. Narongthong et al. studied CB-filled styrene–butadiene rubber (SBR)[30,31] and found that adding the IL 1-decyl 3-methyl imidazolium chloride increased both the electrical conductivity and the electrical response under strain of the composites. The authors argued that the IL improved filler dispersion and increased the number of conductive paths but did not analyze the interactions between the fillers, rubber matrix, and IL.

It remains unclear how the addition of IL to CECs changes the formation of the conducting networks and their

L. Zhang, D. S. Schmidt, L. González-García, T. Kraus
INM – Leibniz Institute for New Materials
Campus D2 2, 66123 Saarbrücken, Germany
E-mail: lola.gonzalez-garcia@leibniz-inm.de; tobias.kraus@leibniz-inm.de
T. Kraus
Colloid and Interface Chemistry
Saarland University
66123 Saarbrücken, Germany

The ORCID identification number(s) for the author(s) of this article can be found under https://doi.org/10.1002/admt.202101700.

DOI: 10.1002/admt.202101700

changes under strain. More in general, there are only a few studies on the microscopic effects of the IL on filler–polymer interfaces. Abraham et al. studied the effect of the IL 1-benzyl-3-methylimidazolium chloride on functionalized multiwalled carbon nanotube (f-MWCNT)-SBR nanocomposites and explained the reinforcement with increased filler–polymer interactions due to better dispersion of the nanotubes in the SBR matrix and a larger interfacial area. However, the authors did not address electrical conductivity.[32] Laskowska et al. added two types of imidazolium ILs to nitrile rubber filled with the non-conductive silica Aerosil 380.[33] The hydrophilic IL increased the ionic conductivity and reduced the tensile strength from 18.8 to 14.6 MPa. The hydrophobic IL enhanced ionic conductivity without deteriorating tensile strength.

This contribution focuses on the effect of IL on the strain-dependent electrical conductivity of CB-filled PDMS. We combined microscopic analysis with macroscopic material testing and assessed the effects of [EMIM][TFSI], an IL that is known not to poison the cross-linking agents used for PDMS[29] but is structurally likely to interact with the surface of a commonly used CB. We found that the addition of the IL compensated for the increase of elastic modulus upon addition of the CB, while the electrical conductivity of the composites was decreased from 1.84 to 0.67 S m^{-1}, depending on IL concentration. The composite's optical properties and the precursors' rheology were examined to reveal the interaction between the different components and the role of the IL. The optical turbidity of PDMS-IL increased in water, while that of pure PDMS remained low. A rheological study of liquid CB-PDMS-IL mixtures indicated that the IL weakened filler–PDMS interactions.

2. Results and Discussion

We first discuss the mechanical and electrical properties of the composites. **Figure 1**a illustrates the effect of the ionic liquid (IL) on electric conductivity and elastic strength of the composite that we prepared by thoroughly mixing the liquid PDMS precursor with carbon black (CB) at a constant volume fraction of 9% (14.8 wt%) and an increasing amount of the IL (indicated as mass ratio between IL and CB content) before cross-linking (see Experimental Section for further details). Both conductivity and Young's modulus decreased with increasing IL content. The decline of mechanical stiffness with increasing IL content could be either due to a reduced cross-linking density of the PDMS, a change in CB–PDMS interfaces, or a combination of both.

The stress–strain curves of the composites in Figure 1b illustrate that IL addition increases the linear–elastic part to larger strains and increases the strain at break compared to CB composites without IL. The CB filler alone increases the ultimate strength and Young's modulus but lowers the ultimate strain.[34] It is often desirable to obtain CECs with large elongations at break, and the effect of IL on the elongation at break is depicted in Figure 1c. The addition of IL increased the elongation at break from 50% in PDMS-CB-IL-0 to more than 180% in PDMS-CB-IL-2, where the composite had the same value as pure (non-filled) PDMS, while reducing the Young's modulus from 4.27 to 2.52 MPa.

The IL reduced the electrical conductivity of the composite, probably by changing the conductive CB network structure, the contact resistances between the CB particles of the filler, or both.

We further measured the resistance change as a function of strain. **Figure 2**b–d illustrates the maximal changes in resistance and the resistance at zero strain after stretching cycles. All samples

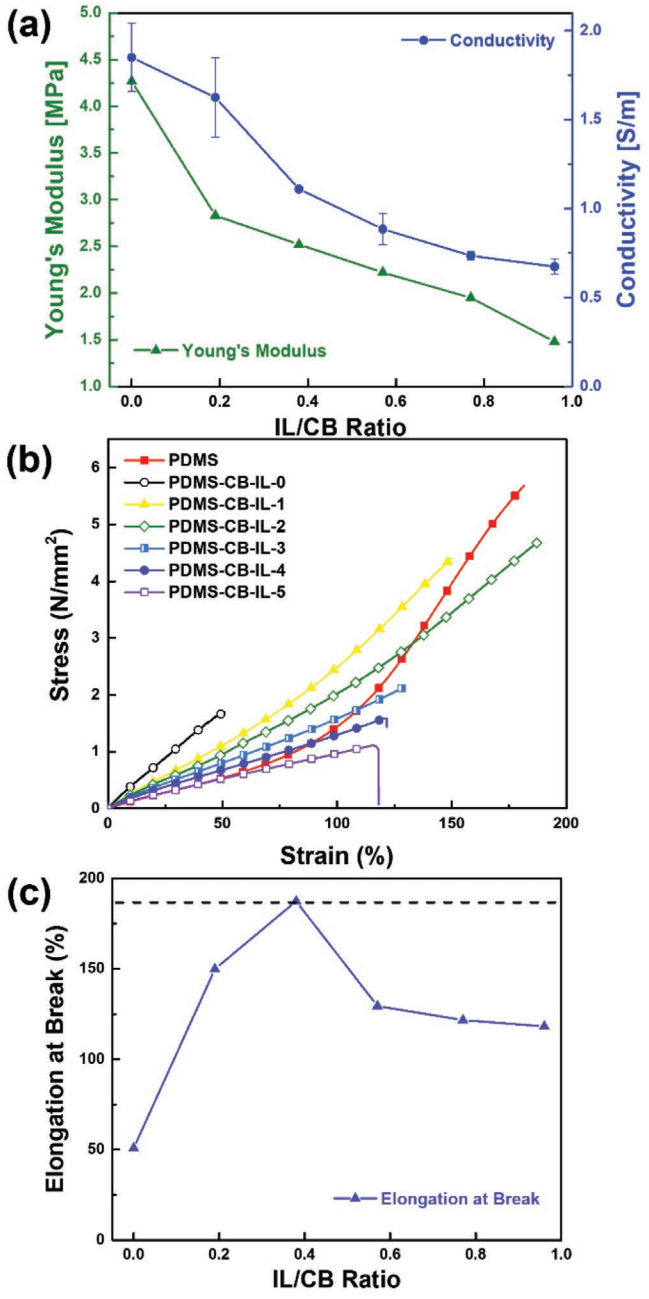

Figure 1. a) Electronic conductivity and elastic strength of PDMS-CB composites with 9% CB fraction and varying IL [EMIM][TFSI] loadings at room temperature. b) Stress–strain curves of PDMS-CB-IL composites with different IL contents. c) Influence of IL on the maximum elongation of as-prepared PDMS-CB-IL composites. The dashed line is the value of elongation of a pure PDMS sample. The standard deviation was obtained with $n = 3$ measurements.

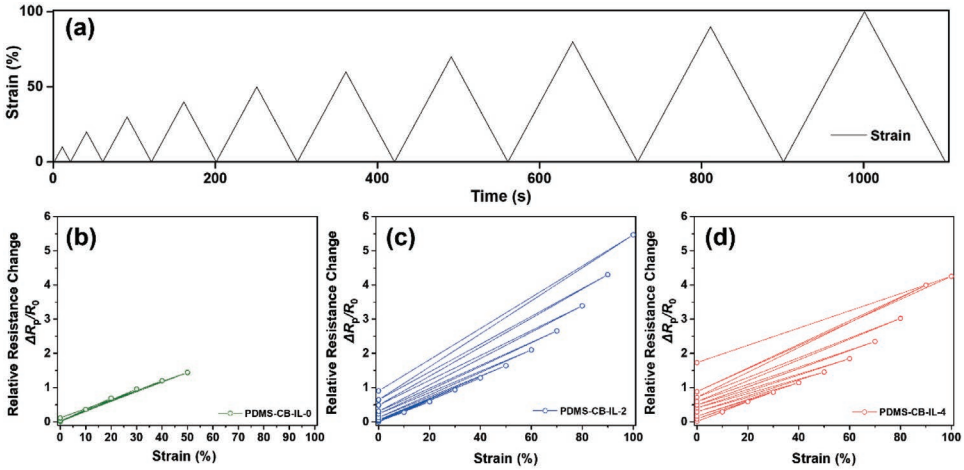

Figure 2. Electrical conductivities of PDMS-CB-IL composites under strain. a) Cyclical strain tests with 10% strain increase per cycle until 100% elongation of samples. PDMS-CB-IL-0 sample underwent five cycles of loading with a strain rate of 1% per second, and PDMS-CB-IL-2 and PDMS-CB-IL-4 sample underwent ten cycles of loadings with a strain of 1% per second. b–d) Relative resistance changes versus strain of the composite samples PDMS-CB-IL-0, PDMS-CB-IL-2, and PDMS-CB-IL-4. The incremental strain was 10% for each cycle, and the resistance was recorded at maximum strain.

underwent five and ten cycles of loading at a strain rate of 1% per second, as shown in Figure 2a. The initial resistance R_0 was taken as the reference for calculating the resistance change for all cycles. The resistance of PDMS-CB-IL-0 composites increased reversibly for strains below 40%, but an irreversible fraction of $\Delta R_p/R_0 \approx 10\%$ remained after straining to 50%. The resistance changes of PDMS-CB-IL-2 composites resembled that of PDMS-CB-IL-0 for strains below 50%, with a slightly increased gauge factor above 30% strain. In summary, the change of resistance at strains below 50% was largely reversible for composites with and without IL, and a large part of it is probably due to the macroscopic change of sample geometries.

Composites without IL failed at strains above 50%. PDMS-CB-IL-2 composites retained an irreversible resistance change after straining beyond 50% and reached approximately $\Delta R_p/R_0 = 1$ at 100% strain. Similarly irreversible changes ($\Delta R_p/R_0 = 2$) have been previously reported for PEDOT:PSS/iTPU samples at 50% strain.[35] Sample PDMS-CB-IL-4 performed similarly to that of PDMS-CB-IL-2 with reduced resistance changes at 100% strain but an increased irreversible component of $\Delta R_p/R_0 = 2$ at the same strain. The irreversible resistance change at strains above 50% indicates a permanent change in microstructure that is exacerbated by larger IL content. It is likely that the overall resistance change above 50% strain is a combination of macroscopic sample deformation and microstructural change.

The strong effects of small IL contents on both mechanical and electrical properties suggest a combination of multiple modes of actions of IL in the composite. In the following, we introduce experiments that help to distinguish IL effects on the polymer matrix, its link to the CB network, the CB network structure, and the electrical contacts between filler particles.

We first analyzed the effect of IL on the PDMS network and performed swelling experiments that probe the cross-linking density of PDMS as a function of IL content. The swelling ratios of water in PDMS without CB and with different amounts of IL are presented in **Figure 3**a. The sample weights after drying M_{ex} were within 99.5% of the initial weights M_0 for all samples. The swelling of PDMS without IL was negligible, and there was no visible change in optical transparency as shown in Figure 3c,d.

The addition of IL to PDMS first increased the swelling ratio up to 13% for PDMS-CB-IL-4 and reduced it to 10% for PDMS-CB-IL-5. Swelling increased the optical scattering in PDMS-IL (Figures 2e,f). The optical effect was reversible and enabled switching between semi-transparent and opaque states by swelling and drying (Figure 2b). We observe that the PDMS-IL-1 sample showed a lower transmittance than the pure PDMS sample before swelling. Our results are consistent with the results of Sinawang et al. who suggested that IL reduces the cross-linking density of PDMS, thus increasing the swelling ratio.[36] This implies that at least a fraction of the IL is molecularly distributed in the entire bulk volume of PDMS.

We analyzed the morphology of the surface and the bulk directly beneath the surface of PDMS and PDMS-IL-1 before and after swelling using optical microscopy (**Figure 4**). Pure PDMS samples did not visibly change after swelling or drying. Figure 4c shows that the addition of IL resulted in the formation of pores directly at the surface. A possible explanation is that the molecular solubility of the IL in PDMS is limited, and a part of it formed a separate phase that is distributed in small droplets. The pores appeared larger after swelling, as shown in Figure 4d. It is likely that the IL droplets create local volumes of low cross-linking densities that strongly swell in the presence of water. Tiwari et al. report that the addition of much larger amounts of IL (10 vol%) leads to the formation of microscopic IL droplets about 1 µm.[37] The droplets that we observe are smaller, but they grow during swelling as water dilutes the (hygroscopic) IL inclusions. This changes the overall swelling behavior of the material. It explains the change of turbidity caused by swelling, because water droplets cause local refractive index contrasts. We did not observe an obvious change in weight of the IL-containing material after swelling and drying, which indicates that the IL remains inside the bulk, with limited leaching, while the water is largely removed during drying.

The mechanical and electrical properties of CB-filled PDMS are strongly affected by the structure that CB forms in the

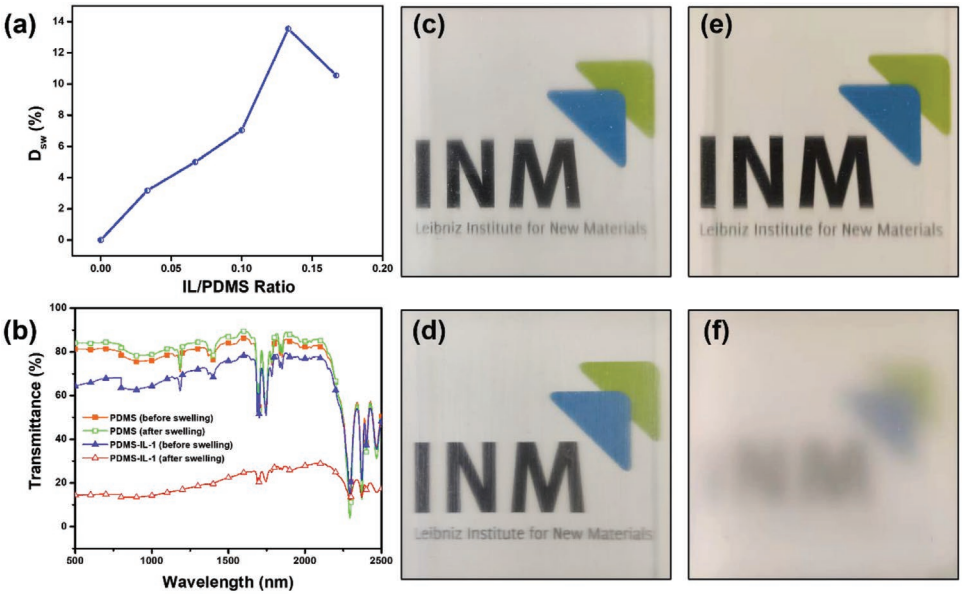

Figure 3. a) Swelling of PDMS with different amounts of the IL [EMIM][TFSI] in water at room temperature. b) Optical transmittance of PDMS and PDMS-IL-1 before and after swelling, respectively. c,d) Optical appearance of PDMS without IL before and after swelling, respectively. e,f) Comparison of PDMS-IL-1 before and after swelling, respectively.

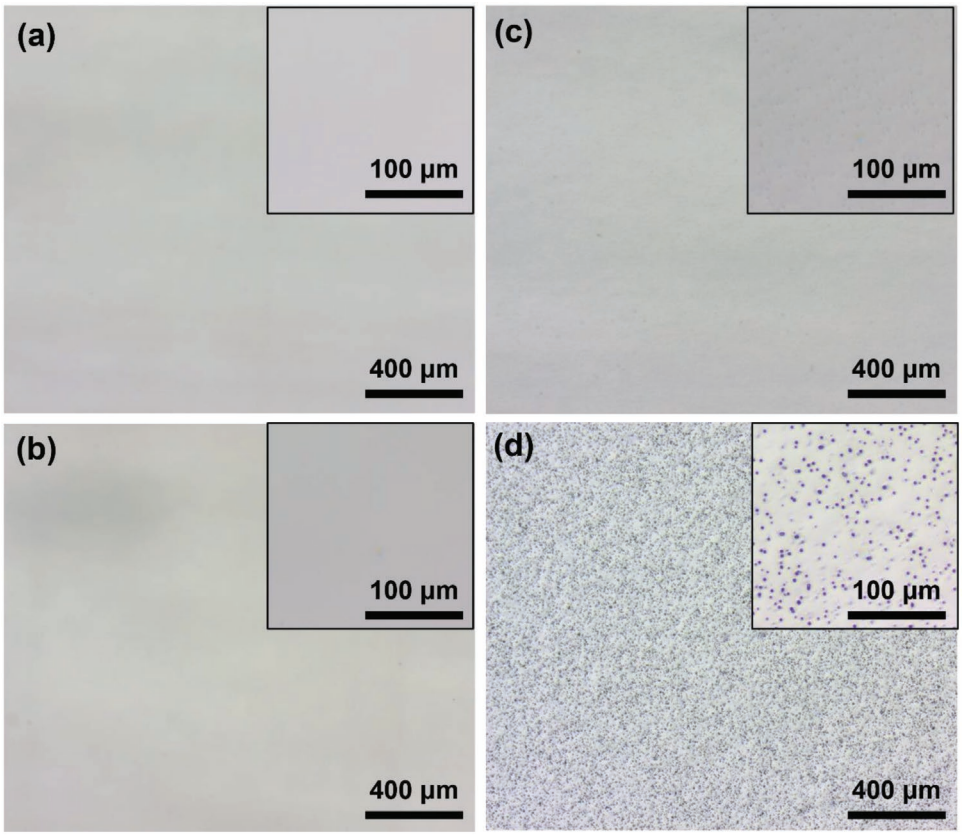

Figure 4. Microstructural effects of water on PDMS and PDMS-IL-1 samples. Optical micrographs of pure PDMS a) in the dry and b) in the swollen state show no visible changes. Optical micrographs of PDMS-IL-1 in c) the dry and d) the swollen state, indicate the formation of pores due to IL addition that grow into droplets upon swelling. All insets are magnifications recorded with a higher-magnification objective.

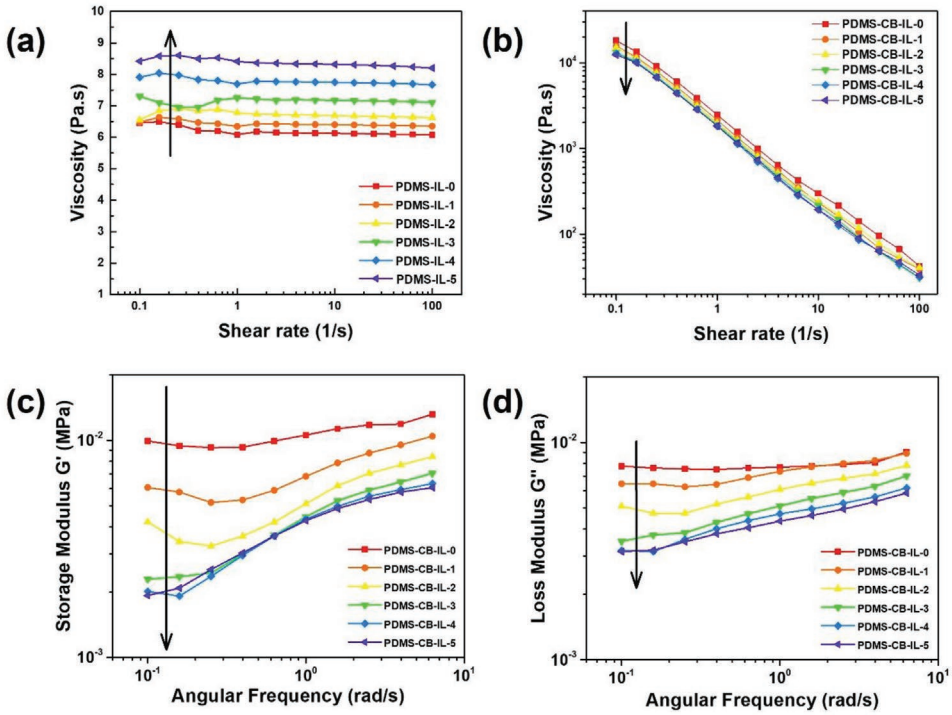

Figure 5. Shear stress and shear viscosity dependence on the applied shear rate of a) PDMS-IL mixtures and b) PDMS-CB-IL composites. Frequency-dependent c) storage and d) loss modulus of PDMS-CB-IL composites.

matrix. Our experiments suggest that the addition of IL alters the interfaces between particles (and thus the gauge factor) and the cross-linking degree of the PDMS matrix. We studied the rheological properties of PDMS-CB-IL precursor mixtures to understand the effect of IL on the interactions between CB aggregates and PDMS and CB. We assume that curing the samples freezes the structure of the viscoelastic precursor but does not change the networks formed by CB. The rheological study above therefore reveals effects of the IL on PDMS and CB that are retained in the solid composites.

Viscosity increased when adding IL to pure PDMS (**Figure 5**a). Marwanta et al. suggested that IL strongly interact with PDMS chains, thus increasing viscosity.[38] We found above that the IL partially forms distributed droplets, which could act as a soft filler that increases viscosity as claimed by Ankit et al.[37] The evolution of the traces shown in Figure 5a are consistent with both mechanisms; the relatively large increase in viscosity at the largest IL contents suggests that the formation of droplets increase viscosity more than the molecular mechanism.

Viscosity, storage, and loss moduli decreased with growing IL content in PDMS-CB-IL mixtures as shown in Figure 5b–d. This opposite trend can be explained with the affinity of the IL towards the non-polar CB fillers that has been reported previously.[33] The fraction of IL that is not soluble in PDMS is likely to adsorb to the CB surface (Figure S1, Supporting Information), thus changing the agglomeration behavior of CB and the solid–liquid hydrodynamics in the mixture. The IL adsorbed at CB–CB interfaces weakens the filler network and the mechanical strength of the agglomerates, and the IL between CB and PDMS reduces the hydrodynamic CB–PDMS coupling (Figure S1, Supporting Information). This is consistent with weakened filler–rubber coupling that was reported for other imidazolium-based ILs previously.[39]

The rheological findings are in good accordance with the results for the solid composites, where an increasing IL content reduced mechanical strength but increased the elongation at break. The stress distribution in PDMS-CB composites with weakened connections between matrix and filler reduces the overall brittleness, and CB fillers with contacts that are "lubricated" by IL are more likely to rearrange when strained (and when the stress is released) than to permanently fracture (Figure S1, Supporting Information). This is consistent with an increased contact resistance between the CB filler aggregates that decreases the overall electrical conductivity with increasing IL content.

3. Conclusion

We prepared CECs with low Young's moduli using an ionic liquid additive and analyzed the mechanisms by which the IL changes the piezoelectric properties of the composites. A combination of swelling experiments, microscopy, and rheology indicated that a part of the IL formed a solid solution in the PDMS, where it reduced the cross-linking density, while a second fraction was dispersed in liquid droplets or adsorbed onto the CB. The resulting reduction in filler–matrix coupling explains the reduction of the elastic modulus and the increased elongation at break.

The IL that adsorbed on the CB probably increased the contact resistance between CB fillers, thus increasing the bulk resistance. More indirectly, it may decrease the tendency to form strong agglomerates, thus decreasing the number of

percolating paths and reducing conductivity, too. Both mechanisms decrease the absolute conductivity but may also reduce the change of conductivity upon strain by making the network less brittle.

The changes in mechanical properties enable the use of the composites as sensors or electrodes for larger range of deformations. The relative changes in resistance upon strain were not much changed by the IL, however. It will be interesting to study other ILs or additional additives that affect the agglomerate network structure more profoundly and compare the results for CB obtained here to anisotropic carbon fillers such as CNTs. Certain applications call for composites with high or low piezoresistive responses that could be engineered by a rational choice of additives.

4. Experimental Section

Sample Preparation: Commercial PDMS Sylgard 184 (Dow Inc.) was used as a polymer matrix and filled with a carbon black (45527, acetylene, 100% compressed, 99.9+%, Alfa Aesar). The ionic liquid [EMIM][TFSI] (Sigma–Aldrich) was tested as additive. Elastomer composites were prepared in two steps to ensure homogeneous mixing. First, fillers, ionic liquid, and the elastomer base were mixed in a SpeedMixer (DAC600.2 VAC-P, Hauschild Engineering, Hamm, Germany) at 2350 rpm under vacuum for 3 min. The volume ratio of CB fillers was fixed at 9 vol% (14.8 wt%) of the final mixture. This CB fraction was larger than the reported percolation threshold of 4.52 vol%.[40] The IL was added at fractions of 0, 0.19, 0.38, 0.57, 0.77, and 0.96 of the CB mass to obtain composites that were named PDMS-CB-IL-0, -1, -2, -3, -4, and -5, respectively. The curing agent was added after mixing all other components and the mixing step was repeated. Finally, the samples were cured at 100 °C for 2 h in the cylindrical mixing jar with a diameter of 33 mm to obtain samples with a thickness of 9 mm.

Samples for tensile testing were prepared in a tensile specimen mold with gauge length of 23 mm, width of 4 mm, and thickness of 2 mm. The mixed slurries were transferred to the tensile specimen mold and cured at 100 °C for 2 h. Samples for swelling experiments were made using simple molds with a size of 30 mm × 7.5 mm × 1 mm and cured at 100 °C for 2 h.

Conductivity: The electronic conductivity of cured bulk samples was measured using the four-probe method with a source meter Keithley 2450 (Tektronix, Inc., USA) at room temperature. The samples were cylinders with diameters of 33 mm and a thickness of 9 mm. The conductivity (σ) of the composites was calculated using the equation

$$\sigma = \frac{1}{2\pi \cdot d} \times \frac{I}{V} \tag{1}$$

where d is the distance between probes, V is the potential difference between the inner probes, and I is the current through the outer probes. Resistance values were recorded while the current was varied from -10^{-5} to 10^{-5} A in 200 steps. A linear fit was used to obtain the conductivity.

Rheology: The rheological properties of the uncured precursor mixtures were characterized with a TA Instruments Discovery HR-3 Rheometer (TA Instruments, USA). Parallel plates with diameters of 20 mm were used at a fixed gap height of 300 µm. Viscosities were measured in rotational mode at shear rates from 0.1 to 100 s^{-1}. Storage and loss modulus were measured in oscillatory mode within the viscoelastic range at oscillation frequencies from 0.1 to 100 rad·s^{-1}. All measurements were done at 25 °C, controlled with a Peltier element.

Swelling and Transmittance: Swelling experiments evaluated the cross-linking density of the composites. Samples with an initial weight M_0 were soaked in de-ionized water for 24 h at room temperature. Excess water was removed with an air gun to obtain the swollen weight M_{sw}. After drying at room temperature for 24 h, the samples had a mass M_{ex}. The degree of swelling, D_{sw}, was calculated as

$$D_{sw} = \frac{M_{sw} - M_{ex}}{M_{ex}} \times 100\% \tag{2}$$

Optical Microscopy: Composite samples were analyzed using a Zeiss AxioScope A.1 light microscope (Zeiss, Germany). All images were taken using reflected light in bright field and recorded with an Axiocam 105 color camera at magnifications of 100 to 500×.

Mechanical Testing: Elastic properties and elongations at break were measured in a universal tensile testing machine Zwick (ZwickRoell GmbH & Co. KG, Germany). Tensile tests were carried out with a strain rate of 1% per second. For the in situ electrical measurements, a Keithley 2450 was connected to the tensile sample with copper foils held in the tensile clamps during testing. The measurement was carried out at a constant current of 10^{-3} A, and the resistance change was recorded every second with the KickStart software.

Statistical Analysis: The statistical data was obtained in a different set of experiments. Samples were prepared and their conductivity was acquired three times (number of measurements $n = 3$). The standard deviation for a single sample was used to estimate the standard error of the mean. The same relative (random) error was then assumed for all conductivity measurements in these experiments. In addition, multiple independent samples were compared and found systematic variations of conductivity from sample to sample at nominally identical compositions, a well-known effect for such composites. Consistency was ensured by choosing one representative sample and showing mechanical and electrical data of the same sample in all graphs.

Supporting Information

Supporting Information is available from the Wiley Online Library or from the author.

Acknowledgements

The authors acknowledge funding by the German Research Foundation in project 404913146. The authors also thank Eduard Arzt for his continuing support of the project. L.G.-G. and D.S.S. acknowledge the European Research Council (ERC) under the European Union's Horizon 2020 research and innovation program (Grant Agreement No. 949785 ELECTROFLUID).

Open access funding enabled and organized by Projekt DEAL.

Conflict of Interest

The authors declare no conflict of interest.

Data Availability Statement

The data that support the findings of this study are available from the corresponding author upon reasonable request.

Keywords

carbon black, cross-linking density, elastomer nanocomposites, elastomers, flexible electrical conductors, ionic liquids, piezoresistivity, swelling

Received: December 22, 2021
Revised: March 18, 2022
Published online: June 16, 2022

[1] M. Nankali, N. M. Nouri, M. Navidbakhsh, N. G. Malek, M. A. Amindehghan, A. M. Shahtoori, M. Karimi, M. Amjadi, *J. Mater. Chem. C* **2020**, *8*, 6185.
[2] Z. Sang, K. Ke, I. Manas-Zloczower, *Composites, Part A* **2019**, *121*, 207.
[3] S. Chen, R. Wu, P. Li, Q. Li, Y. Gao, B. Qian, F. Xuan, *ACS Appl. Mater. Interfaces* **2018**, *10*, 37760.
[4] J. Lee, S. Kim, J. Lee, D. Yang, B. C. Park, S. Ryu, I. Park, *Nanoscale* **2014**, *6*, 11932.
[5] P. Feng, H. Ji, L. Zhang, X. Luo, X. Leng, P. He, H. Feng, J. Zhang, X. Ma, W. Zhao, *Nanotechnology* **2019**, *30*, 185501.
[6] S. Tsuchitani, T. Sunahara, H. Miki, *Smart Mater. Struct.* **2015**, *24*, 065030.
[7] W. Hu, S. N. Zhang, X. Niu, C. Liu, Q. Pei, *J. Mater. Chem. C* **2014**, *2*, 1658.
[8] X. Wang, X. Liu, D. W. Schubert, *Nanomicro Lett.* **2021**, *13*, 64.
[9] A. Larmagnac, S. Eggenberger, H. Janossy, J. Voros, *Sci. Rep.* **2014**, *4*, 7254.
[10] C. B. Karuthedath, U. Fikri, F. Ruf, N. Schwesinger, *Key Eng. Mater.* **2017**, *753*, 18.
[11] J. Chen, J. H. Zheng, Q. W. Gao, J. J. Zhang, J. Y. Zhang, O. M. Omisore, L. Wang, H. Li, *Appl. Sci.* **2018**, *8*, 345.
[12] N. Jiang, D. Hu, Y. Xu, J. Chen, X. Chang, Y. Zhu, Y. Li, Z. Guo, *Adv Compos. Hybrid Mater.* **2021**, *4*, 574.
[13] M. Leboeuf, N. Ghamri, B. Brulé, T. Coupez, B. Vergnes, *Rheol. Acta* **2008**, *47*, 201.
[14] J. K. W. Sandler, J. E. Kirk, I. A. Kinloch, M. S. P. Shaffer, A. H. Windle, *Polymer* **2003**, *44*, 5893.
[15] N. Maity, A. Dawn, *Polymers* **2020**, *12*, 709.
[16] H. Stoyanov, M. Kollosche, S. Risse, R. Wache, G. Kofod, *Adv. Mater.* **2013**, *25*, 578.
[17] T. S. Hansen, K. West, O. Hassager, N. B. Larsen, *Adv. Funct. Mater.* **2007**, *17*, 3069.
[18] L. V. Kayser, D. J. Lipomi, *Adv. Mater.* **2019**, *31*, 1806133.
[19] P. Li, K. Sun, J. Ouyang, *ACS Appl. Mater. Interfaces* **2015**, *7*, 18415.
[20] C. C. Chen, X. T. Bu, Q. Feng, D. G. Li, *Polymers* **2018**, *10*, 1000.
[21] H. W. Liang, Q. F. Guan, Zhu-Zhu, L. T. Song , H. B. Yao, X. Lei, S. H. Yu, *NPG Asia Mater* **2012**, *4*, e19.
[22] M. Wang, R. Li, X. Feng, C. Dang, F. Dai, X. Yin, M. He, D. Liu, H. Qi, *ACS Appl. Mater. Interfaces* **2020**, *12*, 27545.
[23] Y. Kanbur, Z. Küçükyavuz, *J. Reinf. Plast. Compos.* **2009**, *28*, 2251.
[24] A. Das, K. W. Stockelhuber, R. Jurk, J. Fritzsche, M. Kluppel, G. Heinrich, *Carbon* **2009**, *47*, 3313.
[25] J. Fritzsche, H. Lorenz, M. Klüppel, A. Das, R. Jurk, K. Stöckelhuber, G. Heinrich, in *Polymer–Carbon Nanotube Composites*, 1st ed., Elsevier, Amsterdam **2011**, p. 193.
[26] K. Oh, J. Y. Lee, S. S. Lee, M. Park, D. Kim, H. Kim, *Compos. Sci. Technol.* **2013**, *83*, 40.
[27] B. P. Sahoo, K. Naskar, D. K. Tripathy, *Polym. Compos.* **2016**, *37*, 2568.
[28] D. Steinhauser, K. Subramaniam, A. Das, G. Heinrich, M. Klupel, *eXPRESS Polym. Lett.* **2012**, *6*, 927.
[29] S. S. Hassouneh, L. Y. Yu, A. L. Skov, A. E. Daugaard, *J. Appl. Polym. Sci.* **2017**, *134*, 18.
[30] J. Narongthong, A. Das, H. H. Le, S. Wiessner, C. Sirisinha, *Composites, Part A* **2018**, *113*, 330.
[31] J. Narongthong, H. H. Le, A. Das, C. Sirisinha, S. Wiessner, *Compos. Sci. Technol.* **2019**, *174*, 202.
[32] J. Abraham, J. Thomas, N. Kalarikkal, S. C. George, S. Thomas, *J. Phys. Chem. B* **2018**, *122*, 1525.
[33] A. Laskowska, A. Marzec, G. Boiteux, M. Zaborski, O. Gain, A. Serghei, *Polym. Int.* **2013**, *62*, 1575.
[34] H. Peidayesh, K. Mosnáčková, Z. Špitalský, A. Heydari, A. O. Šišková, I. Chodák, *Polymers* **2021**, *13*, 3819.
[35] D. H. Park, H. W. Park, J. W. Chung, K. Nam, S. Choi, Y. S. Chung, H. Hwang, B. Kim, D. H. Kim, *Adv. Funct. Mater.* **2019**, *29*, 1808909.
[36] G. Sinawang, Y. Kobayashi, Y. Zheng, Y. Takashima, A. Harada, H. Yamaguchi, *Macromolecules* **2019**, *52*, 2932.
[37] Ankit, N. Tiwari , F. Ho, F. Krisnadi, M. R. Kulkarni, L. L. Nguyen, S. J. A. Koh, N. Mathews, *ACS Appl. Mater. Interfaces* **2020**, *12*, 37561.
[38] E. Marwanta, T. Mizumo, N. Nakamura, H. Ohno, *Polymer* **2005**, *46*, 3795.
[39] X. Zhang, X. Xue, H. Jia, J. Wang, Q. Ji, Z. Xu, *J. Appl. Polym. Sci.* **2017**, 134.
[40] F. Coupette, L. Zhang, B. Kuttich, A. Chumakov, S. V. Roth, L. González-García, T. Kraus, T. Schilling, *J. Chem. Phys.* **2021**, *155*, 124902.